Electronic Supplementary Material (ESI) for Nanoscale.

Supporting Information

Universal Direct Patterning of Colloidal Quantum Dots by (Extreme) Ultraviolet and Electron Beam Lithography

Christian Dieleman[1], Weiyi Ding[1], Lianjia Wu[2], Neha Thakur[2], Ivan Bespalov[2], Benjamin Daiber[1], Yasin Ekinci[3], Sonia Castellanos [2], Bruno Ehrler[1]**

[1] AMOLF, Center for Nanophotonics, Science Park 104, 1098XG Amsterdam, The Netherlands

[2] Advanced Research Center for Nanolithography, EUV Photoresist Group, Science Park 106, 1098 XG Amsterdam, The Netherlands

[3] Paul Scherrer Institute, Laboratory of Micro and Nanotechnology, Forschungsstrasse 111, 5232 Villigen, Switzerland

Corresponding Author

* Bruno Ehrler: B.Ehrler@amolf.nl, Sonia Castellanos: S.Castellanos@arcnl.nl.

S1. PATTERNED QD FILMS

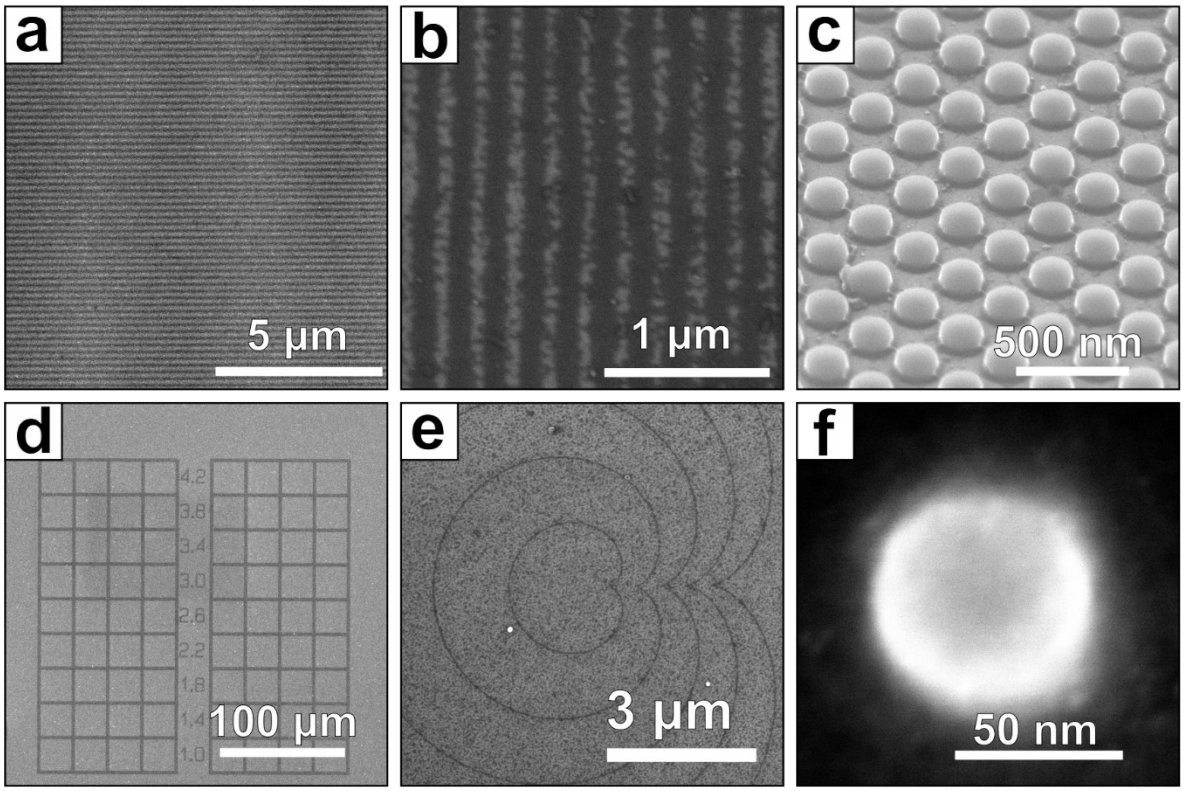

Figure S1. More examples of patterned quantum dot films. (a,b) Lines of PbS quantum dots patterned with EUV, 160 mJ/cm2. (c) PbS quantum dot pillars patterned with EUV, dose 90 mJ/cm2. Development is not complete and some scumming is visible between the pillars. These bridges are in the order of 8 nm. (d) Micron sized straight lines and letters of CdSe. (e) Sub-100 nm curved lines of CdSe CQDs patterned by e-beam lithography, dose 100 µC/cm2. (f) Single pillar of CdSe CQDs patterned by e-beam, dose 100 µC/cm2. All samples are developed with toluene.

S2. AFM OF EUV QD FILMS

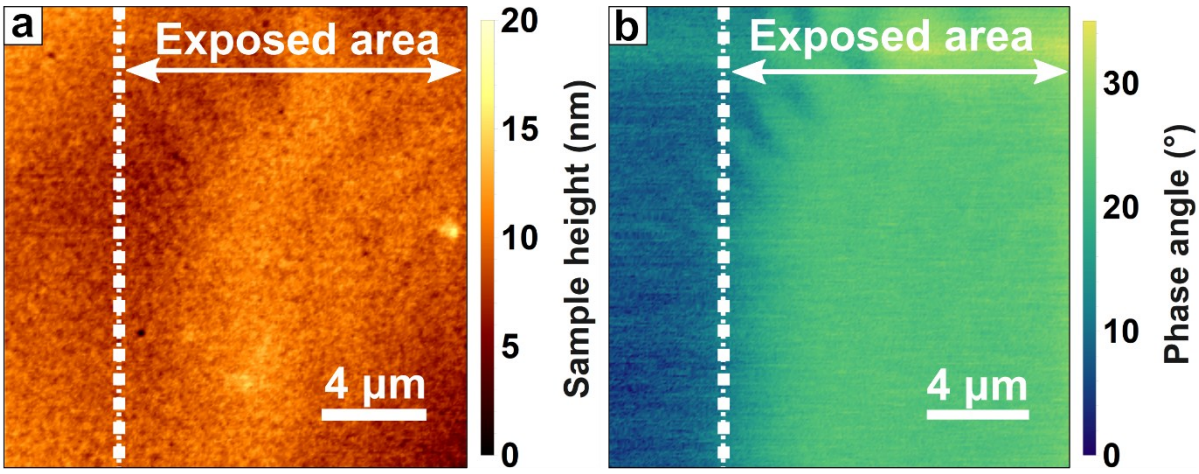

Figure S2. (a) Height map of undeveloped, partially EUV exposed PbS film. Exposed areas (right of the dashed line) show no change in height. **(b)** Phase map of the same film. There is clear contrast in the phase angle between exposed and unexposed regions. The increased phase angle indicates that the exposed area has increased stiffness as compared to the unexposed areas.

S3. EFFECT OF EXPOSURE THRESHOLD IN INTERFERENCE LITHOGRAPHY ON CRITICAL PATTERN DIMENSIONS

The samples that are exposed to Extreme UV are exposed in a synchrotron light source (Swiss Light Source) via interference EUV masks. By interference of 2 or more coherent EUV light beams patterns can be projected on the desired material.[1] A periodic pattern will be formed. There will be a certain intensity slope present between areas of high intensity and areas of low intensity. Preferably this slope is as sharp as possible, to create a precise contrast between intended patterns and intended spaces. In negative photoresists or materials that behave as such, like the quantum dot films we use, a certain density of absorbed EUV photons is required to induce a solubility switch, that will turn the material insoluble in the developer. This dose corresponding to this number of photons is usually designated as D_0. Everywhere on the sample

where this threshold is reached , the material will start to convert into the insoluble product. The features will be very small in cases where only the locations with maximum intensity reach the required number of photons for conversion of the material. By increasing the exposure dose, more and more of the projection field will receive the required dose of photons D_0. When the intensity slope is shallow enough, the printed features will become wider and wider with increasing dose. This principle is demonstrated in **Figure S3**.

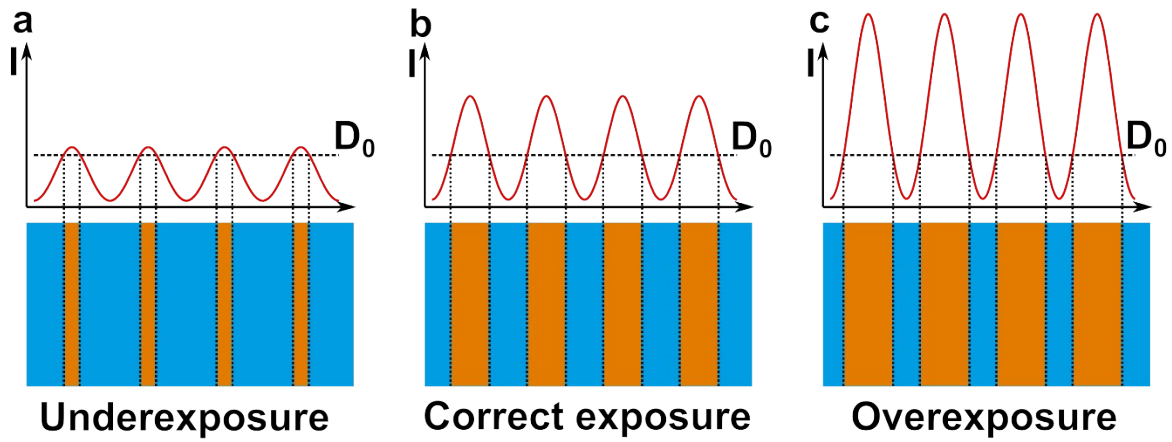

Figure S3. The intensity profile of the projected pattern in interference lithography has a direct influence on the printed features. **(a)** The solubility switch will only occur where the intensity threshold D_0 is reached. **(b)** When the exposure dose is increased and the intensity slope is shallow enough, a larger part of the exposed area will receive the minimum required dose for a solubility switch and the printed features will widen to the correct exposure**. (c)** If the dose keeps increasing the features will widen further and wider features than desired are printed.

S4. CONTRAST

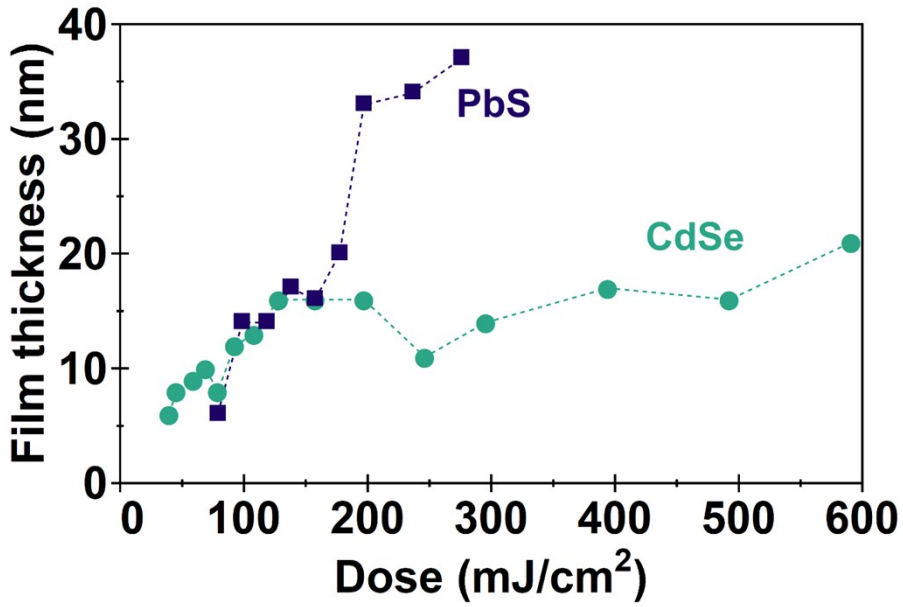

Figure S4. Remaining film thickness of EUV exposed films after development as function of dose. CdSe films start to remain on the substrate at doses as low as 20 mJ/cm^2 (D_0). The remaining film thickness saturates at around 120-150 mJ/cm^2 (D_{100}). Distinct PbS films start to remain on the substrate at doses of around 70 mJ/cm^2 (D_0). At doses around 200-250 mJ/cm^2 the whole film thickness remains (D_{100}).

S5. OPTICAL MICROSCOPE IMAGES OF CONTRAST FIELDS

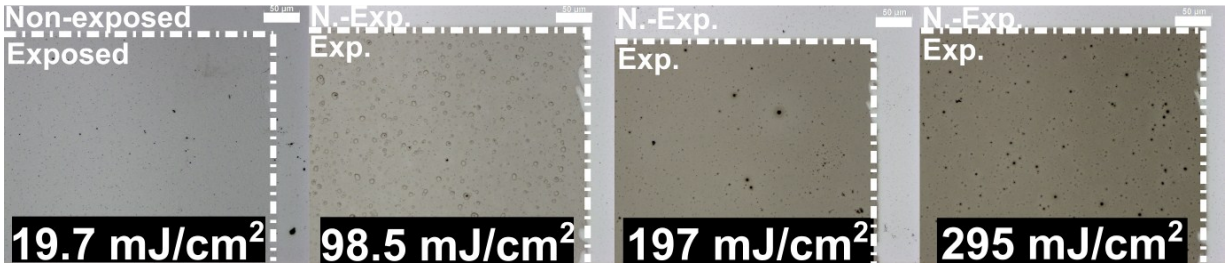

Figure S5. Optical microscope images of EUV exposure fields of CdSe films after development. From doses as low as 10 mJ/cm^2 light contrast can be observed between the exposed and unexposed areas. With increasing dose, the film thickness and with that the visible contrast increases.

S6. QD FILM THICKNESS/PL INTENSITY RELATION

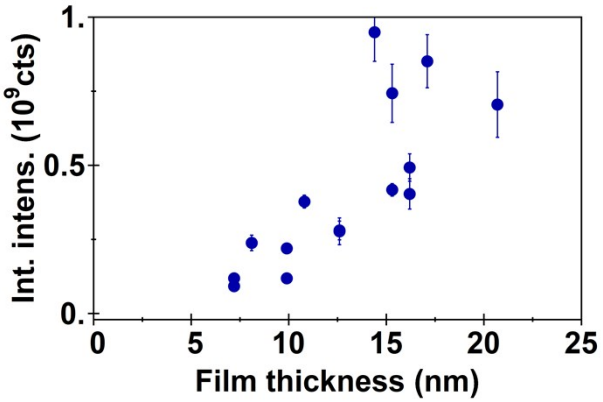

Figure S6. PL intensity as function of film thickness of EUV exposed and developed CdSe films.

S7. FULL WIDTH AT HALF MAXIMUM AS FUNCTION OF SIGNAL-TO-NOISE RATIO

The PL spectra of exposed and developed CdSe films were first normalized and then fitted with a Gaussian profile ($y(x) = \frac{A}{\sqrt{2\pi\sigma^2}} e^{-\frac{(x-\mu)^2}{2\sigma^2}}$ + b.g.) using Mathematica. The normalized spectra can be found in **Figure S7**. Besides the initial redshift of the spectra mentioned in the main text, changes in the spectra are subtle. We do, however, observe a slight narrowing of the linewidth with increasing dose, which is also observed when fitting the spectra, as shown in **Figure S8**.

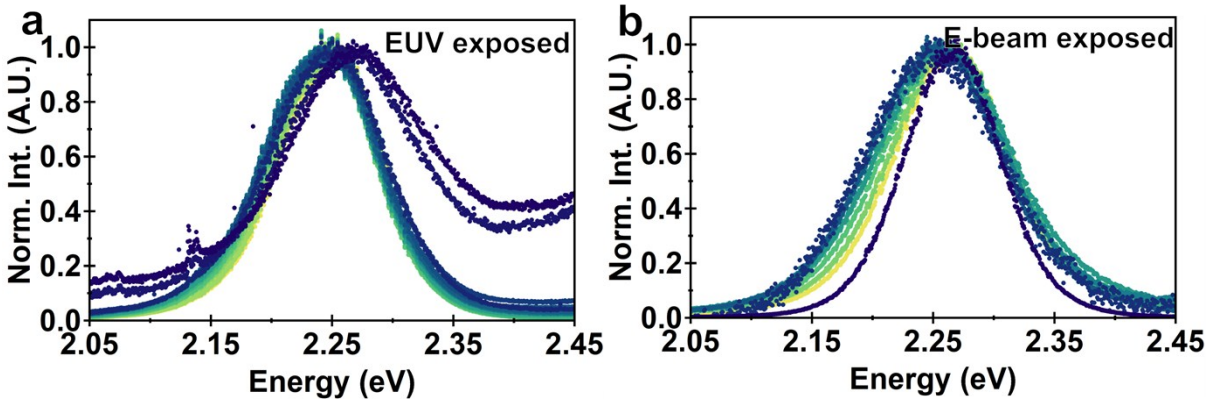

Figure S7. Normalized PL spectra of **(a)** EUV and **(b)** e-beam exposed and developed CdSe films. Lighter colors indicate higher doses. Besides an initial redshift, differences between the spectra are very subtle.

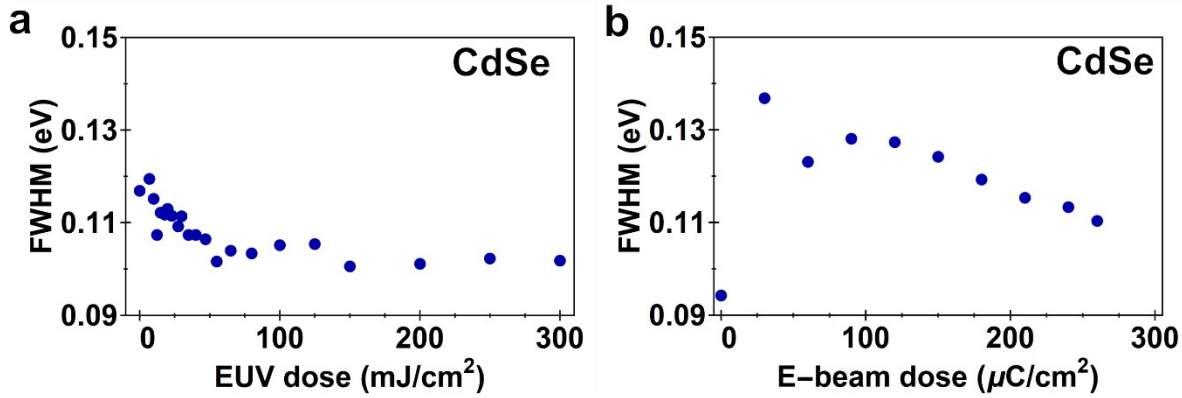

Figure S8. The Full Width at Half Maximum of the PL spectra as fitted for both **(a)** EUV and **(b)** e-beam exposed and developed CdSe films. There is an apparent narrowing of the linewidth with increasing dose.

The full width at half-maximum (FWHM) in both the EUV and e-beam exposed samples decreases as a function of dose, yet the EUV exposed samples plateau at around 80 mJ/cm^2, while the e-beam samples show an initial broadening followed by a constant slope of narrowing. Energy transfer leads to a narrowing in the PL linewidth,[2] however, we attribute the effect of this apparent narrowing to different signal-to-noise ratio of the PL measurements. As mentioned in the main text and shown in **Figure 4**, because lower doses only crosslink part of the film, the fluorescence signal is relatively weak and has hence a low signal-to-noise ratio. When fitting the PL curves, this signal-to-noise level leads to larger fitted peak widths. **Figure S9** shows this effect. We artificially generated Gaussian spectra with random noise of the same amplitude for all spectra. We fixed the peak centers (2.25) and FWHM (0.12), but varied the height of the spectra, thereby varying signal-to-noise (SNR). Subsequently we fitted these spectra with the same fitting routine as used for the fitting of our measured spectra. **Figure S9**a-f show the simulated spectra with the Gaussian fit in red. It is clear that for increasing SNR the fit starts to appear to be more narrow as the base of the curve is not influenced as much by the noise level. **Figure S9**g shows the fitted FWHM value as function of the SNR as well as the actual FWHM used to simulate the spectra. For low SNR the FWHM is grossly overestimated, but when the signal improves, the fit converges on the actual value in a fashion that broadly resembles an inverse square root dependence. At an SNR of 10 the fitted value is still around 9% too high indicating that higher signal-to-noise is preferred. **Figure S9**h shows a similar trend in the fitted FWHM of the measured spectra. When plotted against the measured intensity, the FWHM seems to follow the same inverse square root dependence as the simulated

spectra. We therefore conclude that the observed change in FWHM cannot give us significant information on the physical properties of the nanocrystals.

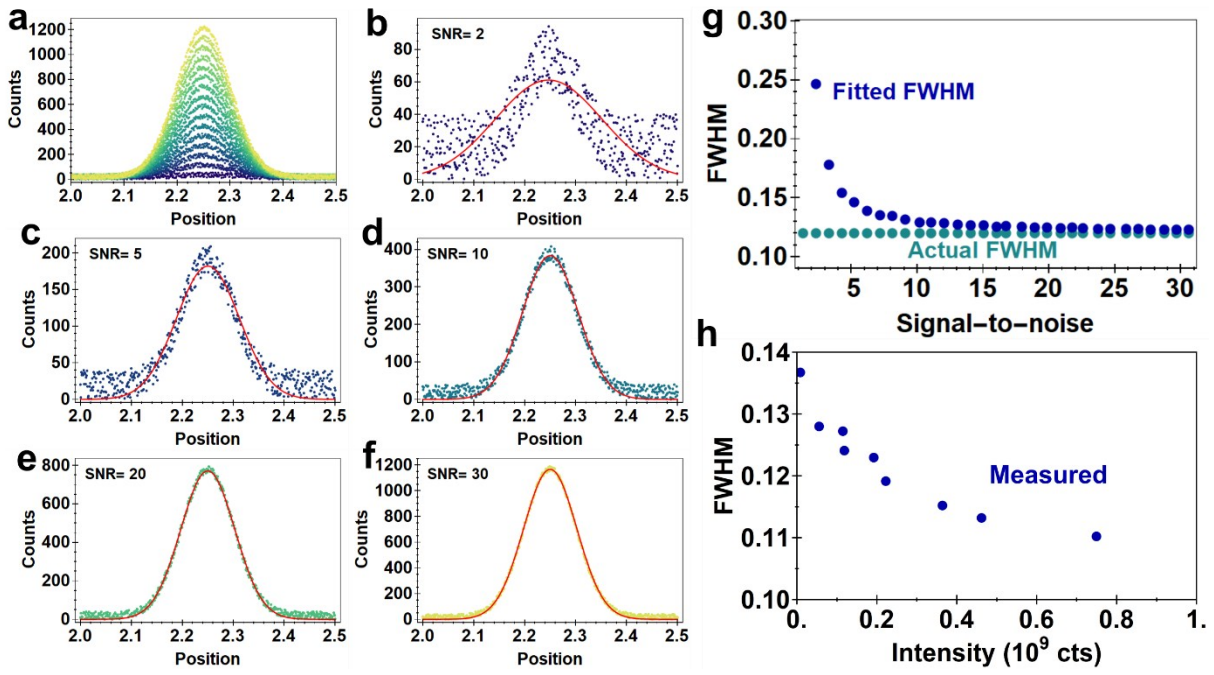

Figure S9. The effect of signal-to-noise on FWHM **(a)** Simulated PL spectra with different signal-to-noise ratios but fixed peak center and FWHM. **(b-f)** Show different spectra with varying SNR from 2 to 30. The red lines indicate the fit. **(g)** Shows the fitted FWHM as function of the signal-to-noise ratio. Errorbars are within every plot point. It is clear that the fitted FWHM depends on the SNR and that the fit converges onto the correct value only when the signal is good enough. **(h)** The fitted FWHM of the measured CdSe PL spectra as function of the integrated intensity. The trend in FWHM is similar as for increased SNR in (g).

S8. STRETCHED EXPONENTIALS OF FITTED LIFETIME CURVES OF EXPOSED CDSE FILMS

As we were probing ensembles of nanocrystals, we found that single or double-exponential fits did not lead to satisfying fits of the lifetime traces. Hence, we fitted the lifetime with 2 terms including one stretched exponential: $y(t) = A_1 e^{-\left(\frac{t}{\tau_1}\right)^{\beta}} + A_2 e^{-\frac{t}{\tau_2}}$. **Figure S10** shows the fitted stretched exponential exponent β of the CdSe quantum dot films exposed to different irradiation sources. A value of β closer to 1 resembles more single-exponent like behavior, while values closer to 0 indicates a more complicated decay from a larger amount of states.[3] For EUV exposed samples we observe a slight initial drop which is consistent with the energy transfer described in the main text. After this initial decrease the exponent is stable at β = 0.29 ± 0.01 for EUV exposure. For e-beam exposure we observe a stable β = 0.36 ± 0.018 over a range of doses.

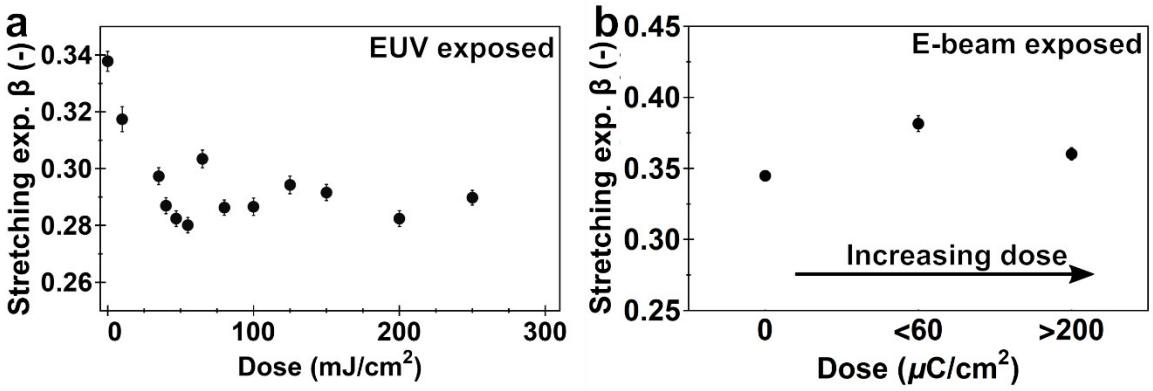

Figure S10. Fitted values of the stretched exponential exponent β of **(a)** EUV exposed and **(b)** e-beam exposed CdSe films.

S9. ESTIMATION OF INTERNAL PHOTOLUMINESCENCE QUANTUM YIELD

We estimate the relative change of PLQY from the internal PLQY, by dividing the rate of emission, by the sum of all rates $PLQY_{int} = \frac{k_{rad}}{k_{total}} \approx \frac{k_{rad}}{k_{rad} + k_{non.rad}}$. This estimate assumes that there are no changes in outcoupling. As we can fit our lifetime data with two exponential terms, with two lifetimes, we can also determine two rates: $k_1 = \frac{1}{\tau_1}$ and $k_2 = \frac{1}{\tau_2}$. We can determine the relative change in PLQY by calculating the ratio of $\frac{k_{rad}}{k_{total}}$. We assume here that τ_1, the long lifetime component is the radiative component and τ_2, the short time component is the non-radiative component, as the radiative lifetimes of CdSe are dominated by slower time components.[4,5] By calculating this measure for PLQY of the sample before exposure and normalizing all the other PLQY values to this value, we can estimate the relative change in PLQY. We can observe that the PLQY decreases after exposure by 20-50%. With e-beam exposure however, we find an increase in PLQY.

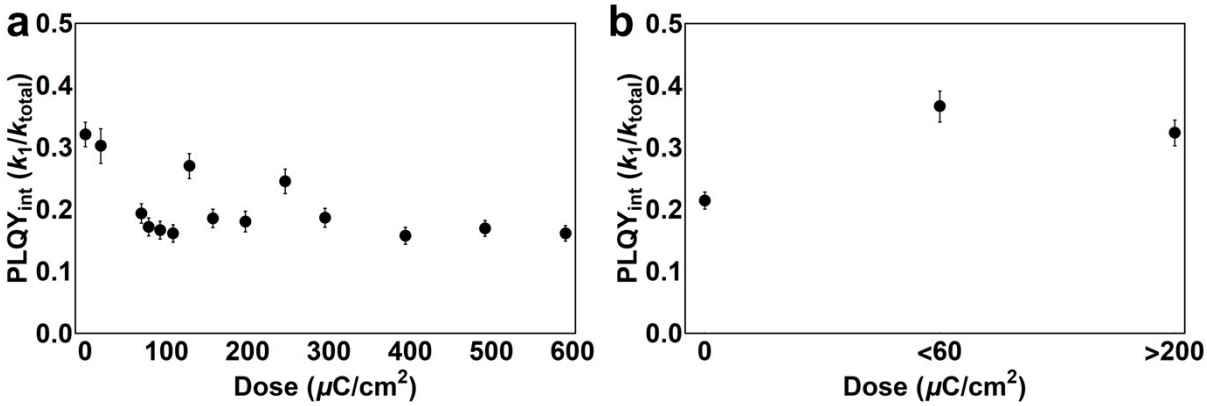

Figure S11. Estimated internal photoluminescence quantum yield of **(a)** EUV exposed and **(b)** e-beam exposed CdSe films.

S10. LEEM EXPOSED SAMPLES

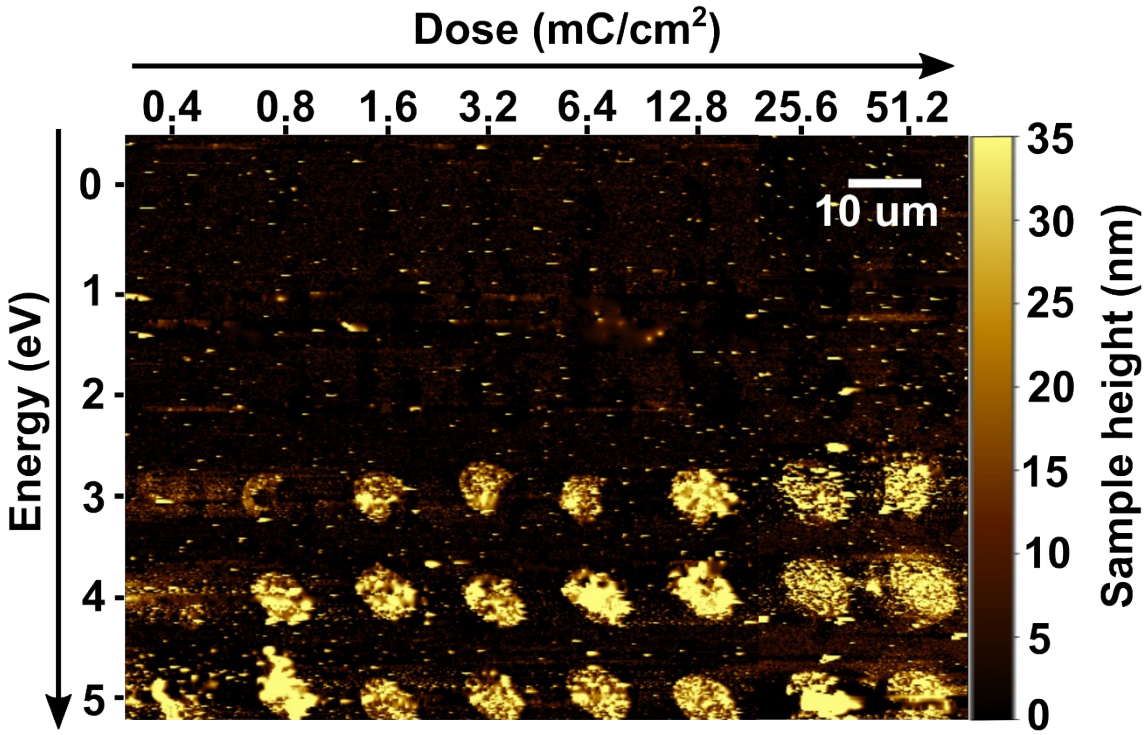

Figure S12. AFM image of dose test of CdSe quantum dots, exposed to Low Energy Electrons of different energy and at different dose. 6 eV electrons can convert the material into an insoluble film.

S11. DUV EXPOSED SAMPLES

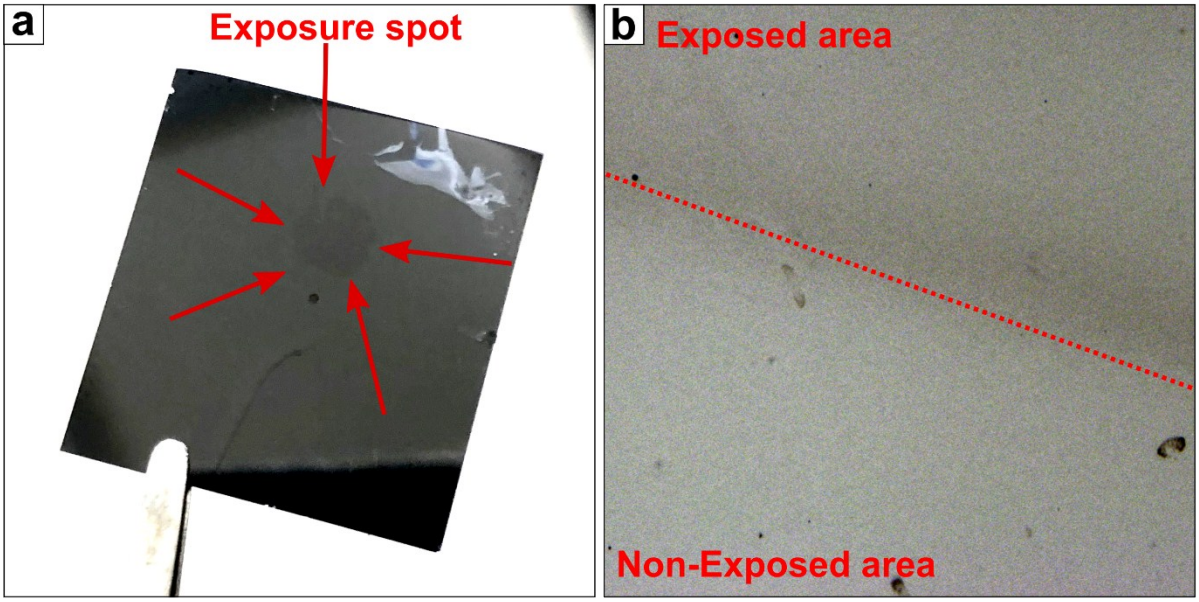

Figure S13. CdSe film exposed to 225 nm DUV and developed in toluene. **(a)** Silicon substrate (19x19 mm) was exposed to 4000 mJ/cm^2 of a 225 nm laser. After development the exposure spot (4 mm diameter) is visible on the substrate, although the remaining film is very thin. **(b)** Optical microscope close up of part of the edge of the exposure spot. Contrast between exposed and unexposed areas is faint, but visible.

REFERENCES

(1) Solak, H. H. Nanolithography with Coherent Extreme Ultraviolet Light. *J. Phys. D. Appl. Phys.* **2006**, *39* (10), R171–R188. https://doi.org/10.1088/0022-3727/39/10/R01.

(2) Kagan; Murray; Bawendi. Long-Range Resonance Transfer of Electronic Excitations in Close-Packed CdSe Quantum-Dot Solids. *Phys. Rev. B. Condens. Matter* **1996**, *54* (12), 8633–8643. https://doi.org/10.1103/physrevb.54.8633.

(3) Schöps, O.; Le Thomas, N.; Woggon, U.; Artemyev, M. V. Recombination Dynamics of CdTe/CdS Core-Shell Nanocrystals. *J. Phys. Chem. B* **2006**, *110* (5), 2074–2079. https://doi.org/10.1021/jp0557013.

(4) Javier, A.; Magana, D.; Jennings, T.; Strouse, G. F. Nanosecond Exciton Recombination Dynamics in Colloidal CdSe Quantum Dots under Ambient Conditions. *Appl. Phys. Lett.* **2003**, *83* (7), 1423. https://doi.org/10.1063/1.1602159.

(5) Gong, K.; Martin, J. E.; Shea-Rohwer, L. E.; Lu, P.; Kelley, D.; F., A. Radiative Lifetimes of Zincblende CdSe/CdS Quantum Dots. *J. Phys. Chem. C* **2015**, *119*, 2231–2238.